Islamic Azad University
Shiraz Branch

Journal of Building Information Modeling
Autumn 2025. Vol 1. Issue 2

https://sanad.iau.ir/journal/bim

Original Research Paper

Flexural Strengthening of Reinforced Concrete Beams with Prestressed L-Shaped Sections: A Numerical Investigation

Mohammad Reza Khastkhodaei* **:** Department of Civil Engineering, Apadana Institute of Higher Education, Shiraz, Iran
Arash Totonchi: Department of Civil Engineering, Apadana Institute of Higher Education, Shiraz, Iran
Seyed Ahmad Jenabali Jahromi: Department of Civil Engineering, Apadana Institute of Higher Education, Shiraz, Iran
Abdelouahed Tounsi: Material and Hydrology Laboratory, University of Sidi Bel Abbes, Faculty of Technology, Civil Engineering Department, Algeria; Department of Civil and Environmental Engineering, King Fahd University of Petroleum & Minerals, 31261 Dhahran, Eastern Province, Saudi Arabia

ARTICLE INFO

Received: 2025/08/07
Accepted: 2025/09/27
PP: 1-14

Use your device to scan and read the article online

Keywords:
Strengthening; Reinforced Concrete; Prestressed Concrete Beam; Flexural Strength; Numerical Modeling; Finite Element Method. .

Abstract

This study introduces and numerically validates a novel method for the flexural strengthening of reinforced concrete (RC) beams using prefabricated, L-shaped prestressed concrete sections. A Finite Element model was developed in Abaqus and validated against existing experimental data for an unstrengthened RC beam. A comprehensive parametric study was then conducted to assess the performance of the strengthened system, focusing on the effects of prestress level and tendon arrangement. The results demonstrate the exceptional efficacy of the proposed technique. The beam's flexural capacity was significantly increased, with the optimal configuration showing a 428.7% enhancement in yield moment compared to the reference beam. Furthermore, the method substantially improves the structure's ductility and energy dissipation capacity, with inelastic energy dissipation increasing by up to 59.9% and damage-related energy dissipation by up to 191%. A direct comparison revealed that the proposed method's performance is approximately 2.5 times greater than strengthening with advanced Ultra-High Performance Fiber Reinforced Concrete (UHPFRC) jackets. This numerical proof-of-concept confirms that the proposed technique is a highly promising and efficient solution for structural retrofitting.

Citation: Khastkhodaei, M. R., Totonchi, A., Jenabali Jahromi, S. A., & Tounsi, A. (2025). **Flexural Strengthening of Reinforced Concrete Beams with Prestressed L-Shaped Sections: A Numerical Investigation**. *Journal of Building Information Modeling*, 1(2), 1-14. https://doi.org/10.82485/bim.2025.1217117

* Corresponding author: Mohammad Reza Khastkhodaei, Email: m.khastkhodaei@live.com

INTRODUCTION

Concrete is one of the most widely used construction materials globally due to its economic advantages and the accessibility of its raw materials (Al Khaffaf et al., 2025; Althoey et al., 2023; Favier et al., 2018). It is utilized in a vast array of structures, including buildings, bridges, dams, and offshore platforms. While concrete exhibits high compressive strength, it is notably weak in tension. This weakness leads to the formation of cracks under tensile stresses induced by applied loads, shrinkage, or temperature variations. To counteract this, steel reinforcement is embedded within the concrete to carry the tensile forces. An advanced approach involves prestressing, where high-strength steel tendons are tensioned to induce a pre-compressive force in the concrete, thereby delaying the onset of cracking (Nawy, 1988).

Over time, many existing concrete structures suffer from degradation, material fatigue, or exposure to harsh environmental conditions, necessitating repair or strengthening (Mirzaee et al., 2021; Sharif et al., 1994). The need for strengthening also arises from changes in building codes, modifications in the structure's use, or errors during the initial design and construction phases. Consequently, various strengthening techniques have been developed. Common methods for enhancing the seismic resistance and ductility of concrete beams include the application of fiber-reinforced polymer (FRP) jackets, steel jackets or plates, and reinforced concrete (RC) jackets (Attari et al., 2019; Esmaeeli et al., 2015; Gergely et al., 2000; Gkournelos et al., 2021; Hadi & Tran, 2014; Kabashi et al., 2025; Karbhari, 2001; Ma et al., 2017; Raza et al., 2019; Singh & Murty, 2024). While RC jacketing is a traditional and effective method for increasing flexural and shear strength, it has notable drawbacks, such as a significant increase in the member's weight and dimensions, which can reduce usable space and is contrary to the goal of weight reduction in seismic retrofitting (Attari et al., 2019; Shahbazpanahi & Manie, 2006).

Previous research has explored various strengthening techniques. Hassani Tabar *et al*., (Hassani Tabar et al., 2014) experimentally investigated the use of prestressed CFRP plates and found that prestressing improved load-bearing capacity. Similarly, Haji Hashemi studied near-surface mounted (NSM) prestressed CFRP strips, noting an 11.5% to 15% increase in ultimate load capacity for prestressed samples compared to a 10% increase for non-prestressed ones (Hajihashemi, 2008). Lampropoulos *et al.*, (Lampropoulos et al., 2016) explored the use of Ultra-High Performance Fiber Reinforced Concrete (UHPFRC) layers and jackets, finding that a three-sided UHPFRC jacket provided the best performance.

This paper introduces a novel strengthening method using pre-fabricated, prestressed concrete beams. This approach offers several potential advantages over conventional post-tensioning methods that often rely on shotcrete, which is not considered a high-strength concrete. The proposed method benefits from:

- **Quality Control:** The prestressed beams are fabricated in a controlled factory environment, ensuring higher quality compared to on-site methods.
- **Durability:** The high-quality fabrication and strong bond between steel and concrete in pre-tensioned members eliminate the need for periodic inspections and reduce the risk of stress loss over time.
- **Cost-Effectiveness:** The proposed technique is potentially more economical than post-tensioning or FRP-based methods.

Therefore, the primary objective of this paper is to conduct a numerical investigation to establish a proof-of-concept for this novel strengthening technique. A detailed parametric study is performed to quantify its potential benefits and identify key behavioral trends, thereby laying the groundwork for future experimental validation.

Research Methodology

The research process involved numerically modeling a reference RC beam in the Finite Element software Abaqus (Abbassi et al., 2023; Abdolpour & Sawicki, 2025; Al-Ashmawy et al., 2023; Bouakaz et al., 2014; Chen et al., 2023; Elsalakawy et al., 2025; Habibi et al., 2022; He et al., 2025; Islam, 2020; Kim et al., 2025; Laib et al., 2021; Lewiński & Więch, 2020; Mobasseri & Janghorban, 2024; Mobasseri et al., 2022; Mobasseri & Mobasseri, 2016; Mobasseri et al., 2020; Mobasseri et al., 2024; Ni et al., 2025; Sadeghi & Hesami, 2018; Shakor et al., 2021; Tan et al., 2025; Wang et al., 2024) and then simulating its strengthening with the proposed method. A parametric study

was conducted to evaluate the effects of the number of prestressing tendons and the level of prestress.

Reference Model

The reference model for this study is based on the experimental work detailed in Lampropoulos *et al*., (Lampropoulos et al., 2016) which serves as the validation benchmark. The base RC beam has a cross-section of 150 mm × 250 mm and a total length of 2200 mm, with an effective span of 2000 mm. It is reinforced with two 12 mm diameter steel bars in the tension zone, having a yield strength of 500 MPa and a concrete cover of 25 mm. The 28-day cylindrical compressive strength of the concrete is 39.5 MPa. The beam was subjected to a four-point bending test. Details of the base model beam are shown in Figure 1 and the experimental setup is depicted in Figure 2.

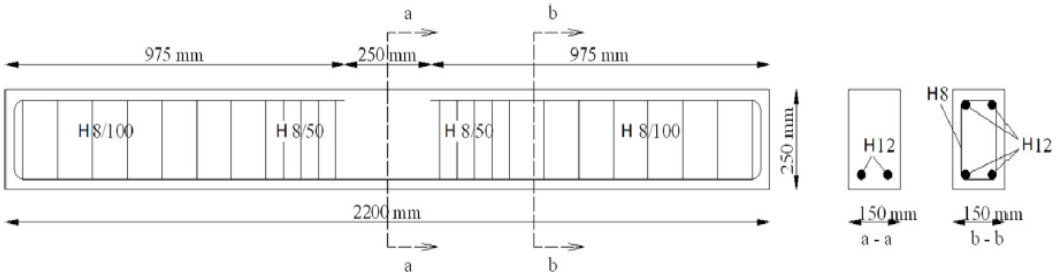

Fig 1. Base Model

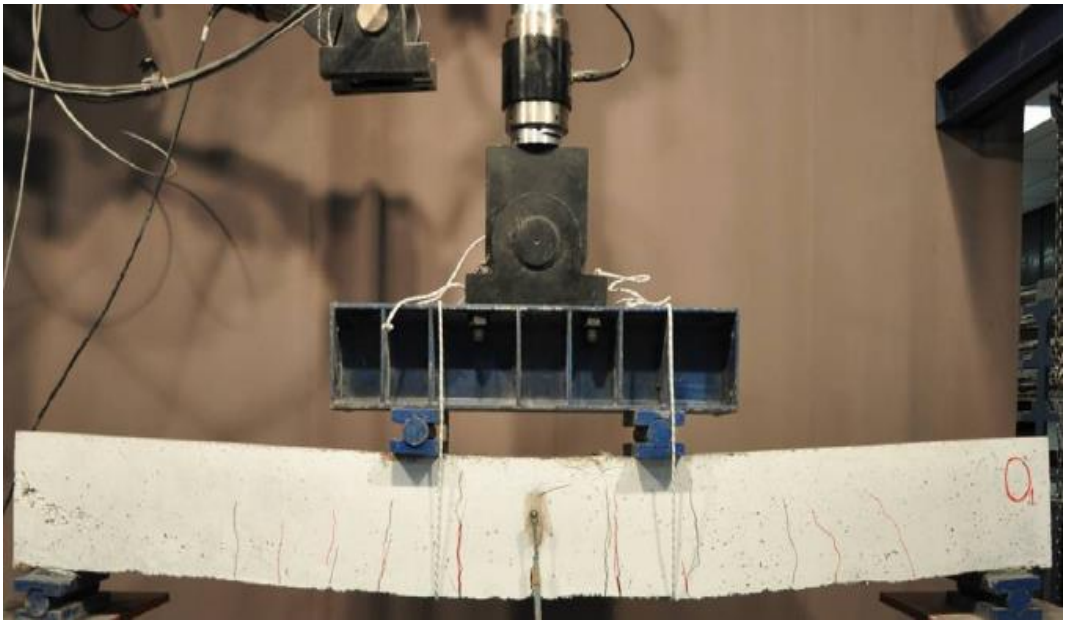

Fig 2. Experimental Setup

Numerical Modeling

All simulations were performed using ABAQUS software (v.2016) (Abbassi et al., 2023; Mobasseri & Janghorban, 2024; Mobasseri et al., 2022; Mobasseri & Mobasseri, 2016; Mobasseri et al., 2020; Mobasseri & Soltani, 2013; Mobasseri et al., 2024; Systèmes, 2016). The analysis was conducted using a Dynamic Explicit step over a duration of 80 seconds.

Component Modeling (Part Module)

All components, including the main RC beam, the L-shaped strengthening beams, reinforcing bars, and prestressing tendons, were modeled as 3D deformable parts. The loading and support plates were modeled as 3D discrete rigid bodies to prevent deformation during analysis. A view of the modeled RC beam is shown in Figure 3, the reinforcement cage in Figure 4, and an L-shaped strengthening beam in Figure 5.

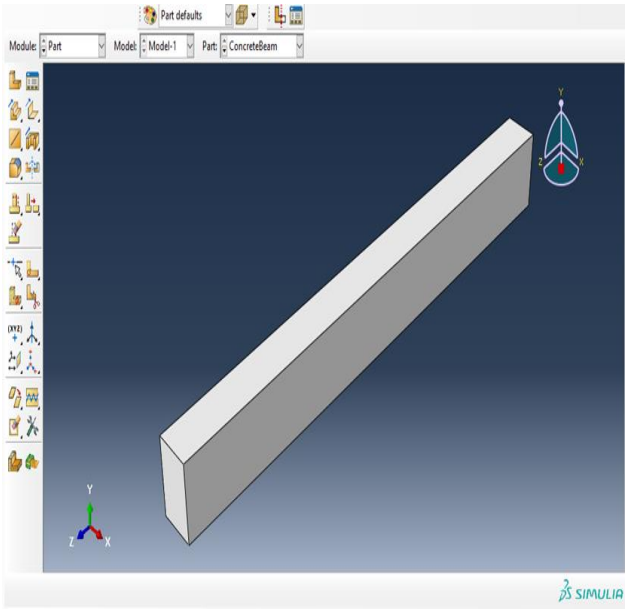

Fig 3. Modeled RC Beam

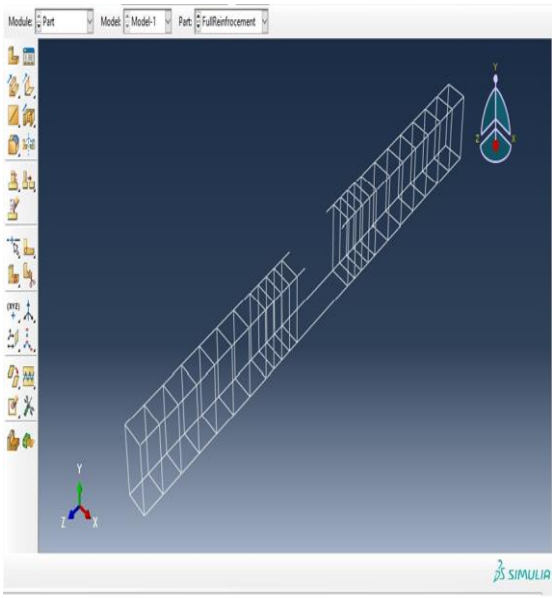

Fig 4. Reinforcement Cage

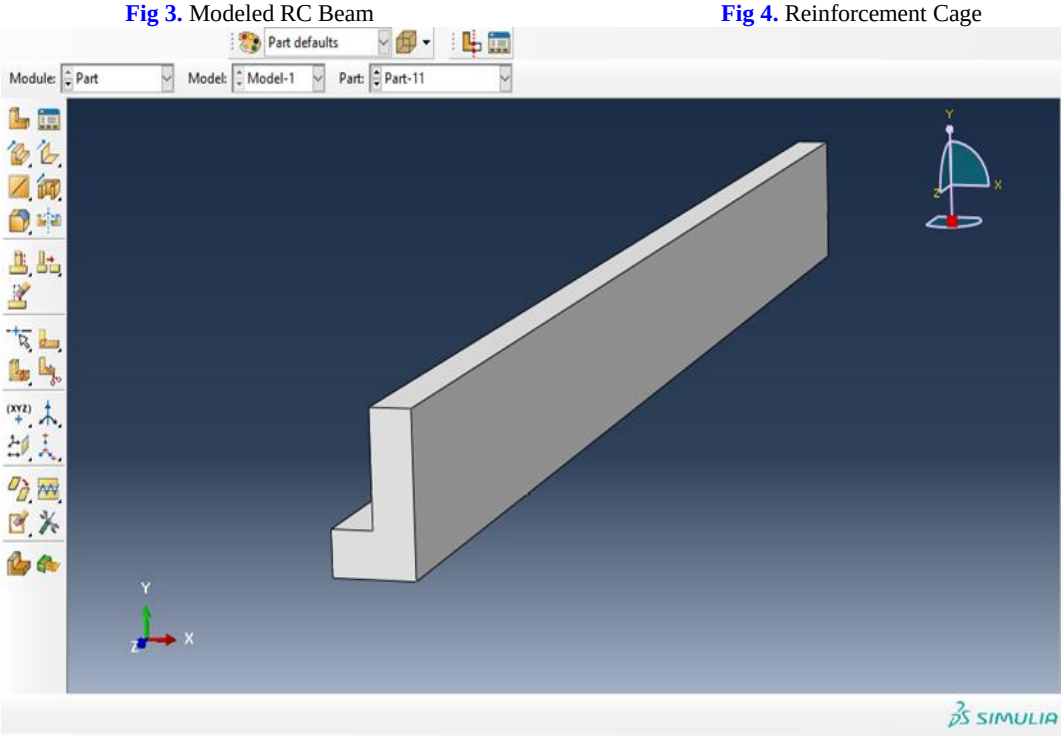

Fig 5. L-shaped Strengthening Beam

Material Properties (Property Module)

Concrete: The concrete was modeled using the Concrete Damage Plasticity (CDP) model. The material parameters were based on the reference paper and relevant literature (Jankowiak & Lodygowski, 2005; Sümer & Aktaş, 2015). The density, Young's modulus, and Poisson's ratio were defined as per Table 1. The specific parameters for the CDP model, including compressive behavior and damage evolution, are illustrated in Figures 6, 7, and 8. A single concrete type (C40) was used for both the main beam and the strengthening beams.

Table 1. Concrete Parameters

Density ($tonne/mm^3$)	Young's modulus (MPa)	Poisson's ratio
2.5e-09	36000	0.2

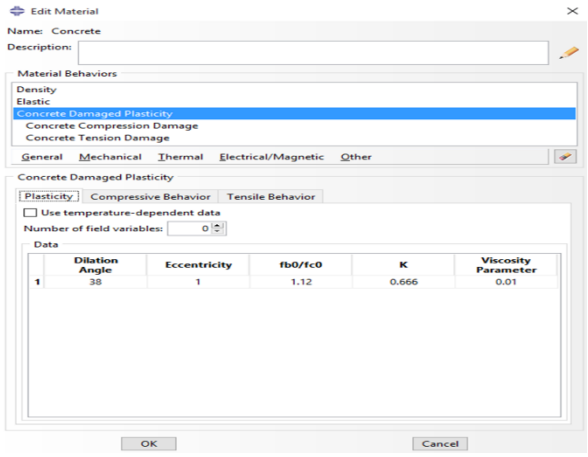

Fig 6. Specific Parameters for CDP Model

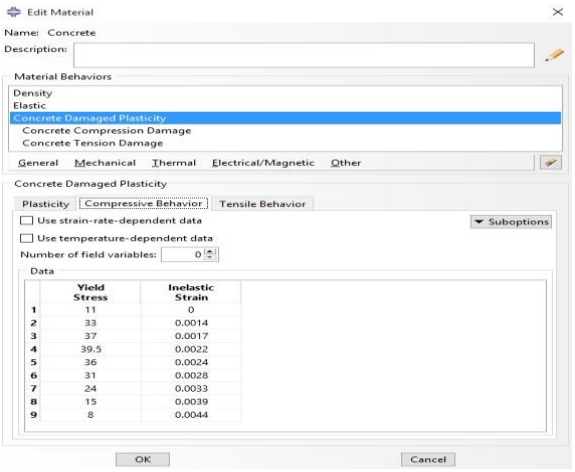

Figu 7. Concrete Compressive Behavior

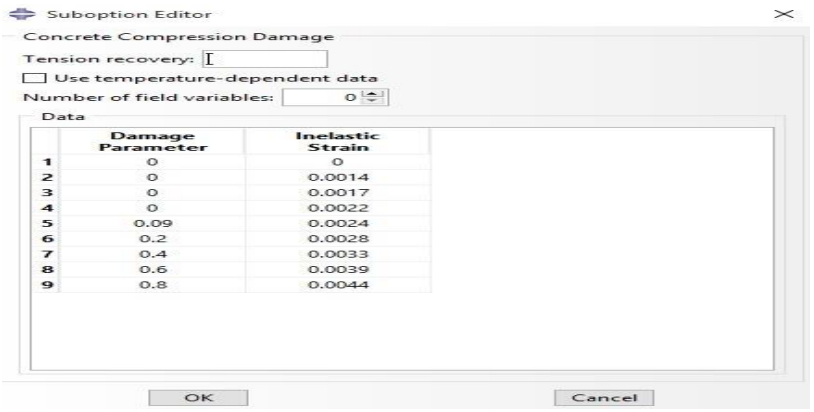

Fig 8. Concrete Compressive Damage Evolution

Steel Reinforcement: The reinforcing steel was modeled with properties as listed in Table 2, with a specified yield strength of 500 MPa.

Table 2. Reinforcing Steel Properties

Density ($tonne/mm^3$)	Young's modulus (MPa)	Poisson's ratio
7.85e-09	205000	0.3

Prestressing Tendons: The tendons were modeled based on the ASTM A416 standard for low-relaxation, Grade 270 strands (International, 2018), with a nominal diameter of 9.53 mm. Their mechanical properties are given in Table 3.

Table 3. Grade 270 Strands Properties

Density ($tonne/mm^3$)	Young's modulus (MPa)	Poisson's ratio
7.85e-09	196508	0.3

Assembly and Interactions

The individual parts were assembled to create the final model, as shown in Figure 7. A perfect bond was assumed between the strengthening beams and the main RC beam by using a tied interface. This assumption was made to evaluate the theoretical maximum performance of the fully composite section and to isolate the effects of the prestressing parameters. The analysis of interfacial slip and the design of shear connection mechanisms are complex issues that are considered beyond the scope of this initial proof-of-concept study and are recommended for future experimental investigation. Reinforcing bars and prestressing tendons were embedded within the concrete host regions using the "Embedded Region" constraint, as shown for the rebar in Figure 8. A general contact algorithm was used for all other interactions.

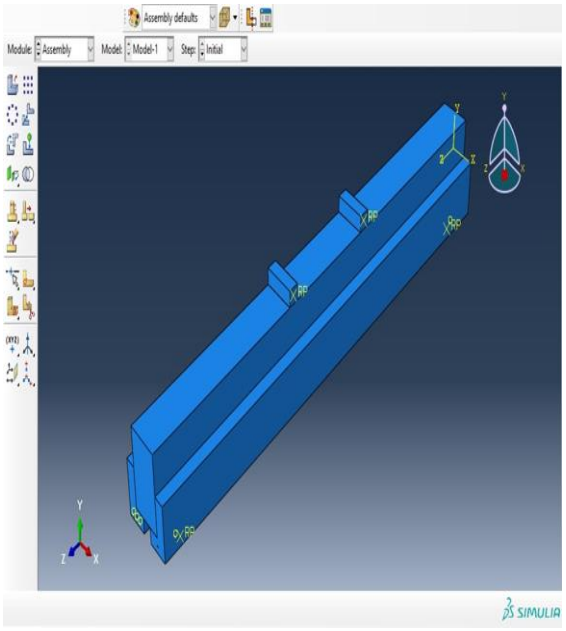

Fig 9. Assembled Model

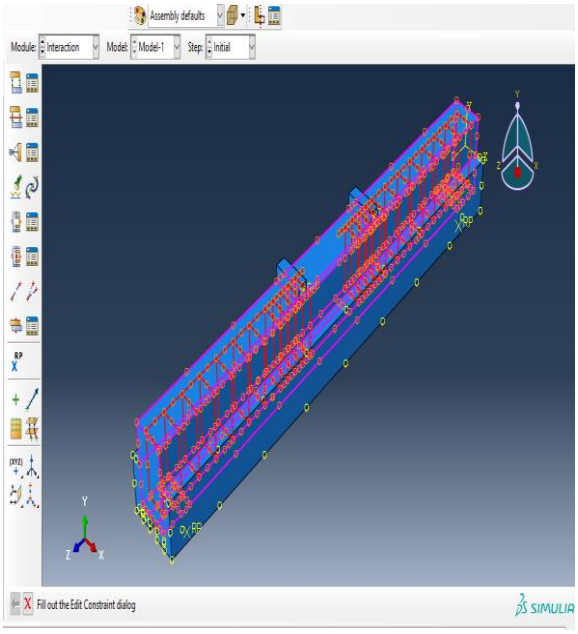

Fig 10. Embedded Region Constraint

Loading and Boundary Conditions (Load Module)

The simulation was displacement-controlled to replicate the experimental test. A vertical displacement was applied to the top loading plates at a rate of 0.5 mm/s, up to a total of 40 mm. This is depicted in 9 and 10. The prestressing force was applied to the tendons as an initial stress condition using the "Predefined Field" option, as shown in Figure 11.

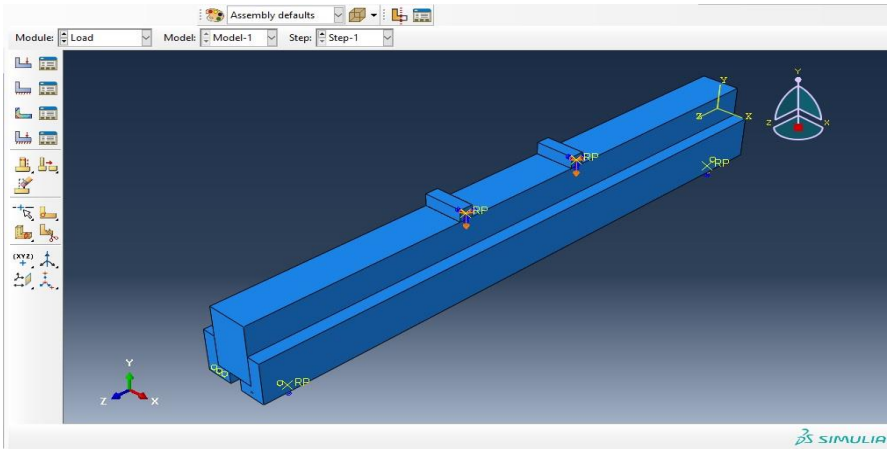

Fig 11. Applied Vertical Displacement in Model

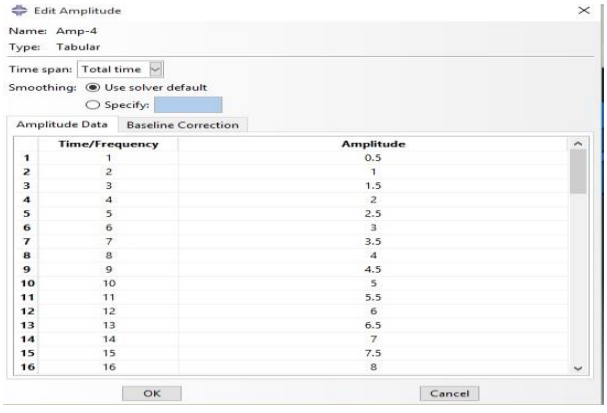

Edit Amplitude

Name: Amp-4
Type: Tabular
Time span: Total time
Smoothing: Use solver default
Specify:

Amplitude Data | Baseline Correction

	Time/Frequency	Amplitude
1	1	0.5
2	2	1
3	3	1.5
4	4	2
5	5	2.5
6	6	3
7	7	3.5
8	8	4
9	9	4.5
10	10	5
11	11	5.5
12	12	6
13	13	6.5
14	14	7
15	15	7.5
16	16	8

OK Cancel

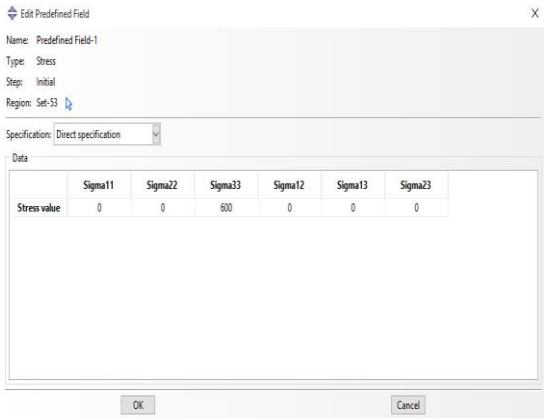

Edit Predefined Field

Name: Predefined Field-1
Type: Stress
Step: Initial
Region: Set-53
Specification: Direct specification

Data

	Sigma11	Sigma22	Sigma33	Sigma12	Sigma13	Sigma23
Stress value	0	0	600	0	0	0

OK Cancel

Fig 12. Applied Vertical Displacement Data

Fig 13. Initial Stress Condition in Predefined Field

Parametric Study and Naming Convention

A total of 10 models were analyzed. The unstrengthened beam is named Base. The strengthened models were organized into three series based on the number of prestressing tendons (1, 2, or 3) and three levels of total prestress (300, 600, or 900 MPa). The naming convention is detailed in Table 4. For instance, model 2s-600 refers to a beam strengthened with two tendons, each carrying a stress of 300 MPa, for a total equivalent stress of 600 MPa. Visual representations of the different strengthened models are provided in Figures 12, 13, and 14.

Table 4. Models Naming Convention

Model Name	Description
Base	**Unstrengthened beam**
1S-300	Strengthened Beam with one tendon, carrying a stress of 300 MPa
1S-600	Strengthened Beam with one tendon, carrying a stress of 600 MPa
1S-900	Strengthened Beam with one tendon, carrying a stress of 900 MPa
2S-300	Strengthened Beam with two tendons, each carrying a stress of 150 MPa
2S-600	Strengthened Beam with two tendons, each carrying a stress of 300 MPa
2S-900	Strengthened Beam with two tendons, each carrying a stress of 450 MPa
3S-300	Strengthened Beam with three tendons, each carrying a stress of 100 MPa
3S-600	Strengthened Beam with three tendons, each carrying a stress of 200 MPa
3S-900	Strengthened Beam with three tendons, each carrying a stress of 300 MPa

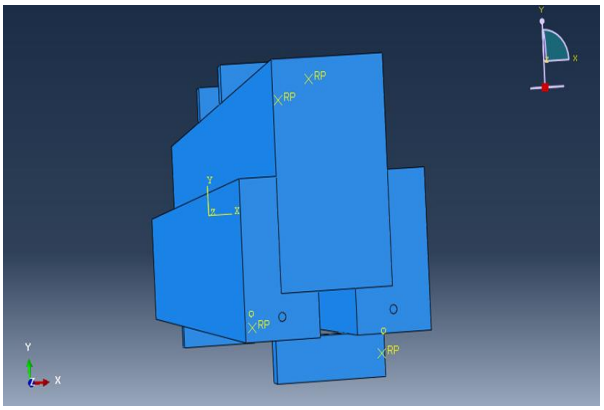

Fig 14. 1S Models

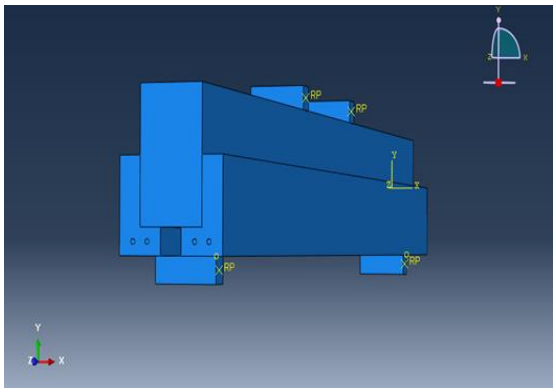

Fig 15. 2S Models

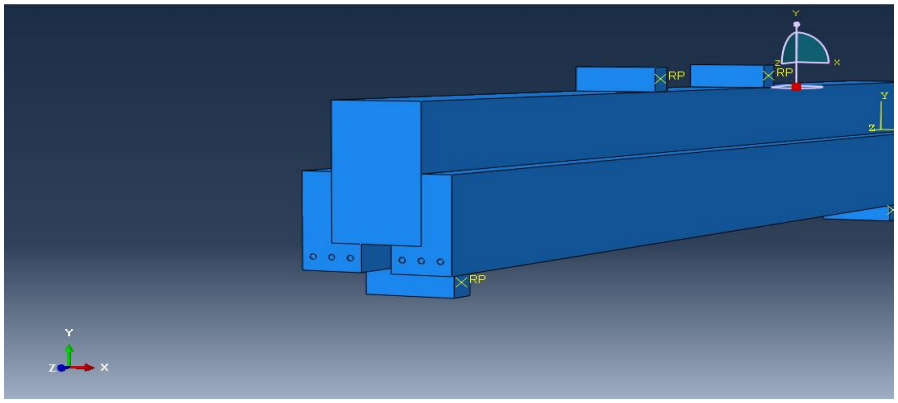

Fig 16. 3S Models

Model Validation

Verification of the Base Model

The first step was to validate the numerical model by comparing the simulation results of the Base model with the experimental (IBexp) and numerical (IBnum) results from the reference paper (Lampropoulos et al., 2016). As shown in Figure 15, the load-deflection curve of the Abaqus model shows good agreement with the benchmark data. The maximum error of the Abaqus model relative to the experimental results was approximately 2.5%,

whereas the error in the reference paper's numerical model was 3.9%. This level of accuracy was deemed sufficient for proceeding with the parametric study.

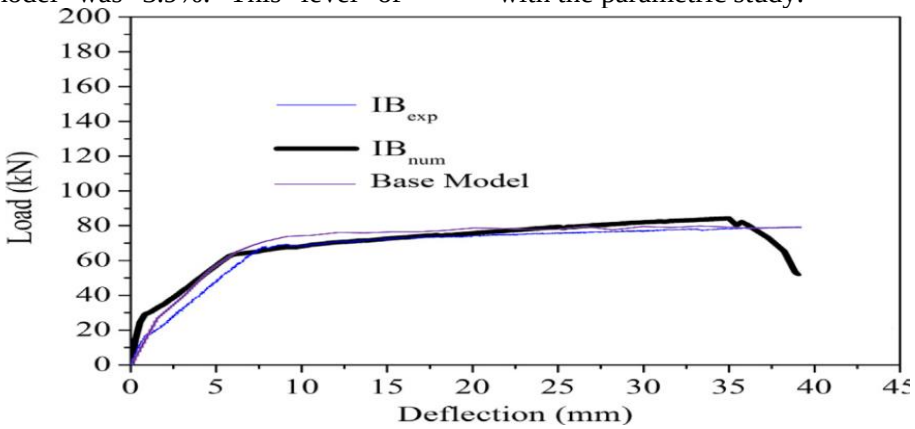

Fig 17. Verification of the Base Model

Mesh Sensitivity Analysis

To ensure the results were independent of mesh size, a sensitivity analysis was performed using three different mesh sizes: 40 mm, 50 mm, and 60 mm. The resulting load-deflection curves are plotted in Figure 17. As the results showed convergence, the 50 mm mesh size was selected as the optimal choice, providing a balance between accuracy and computational cost.

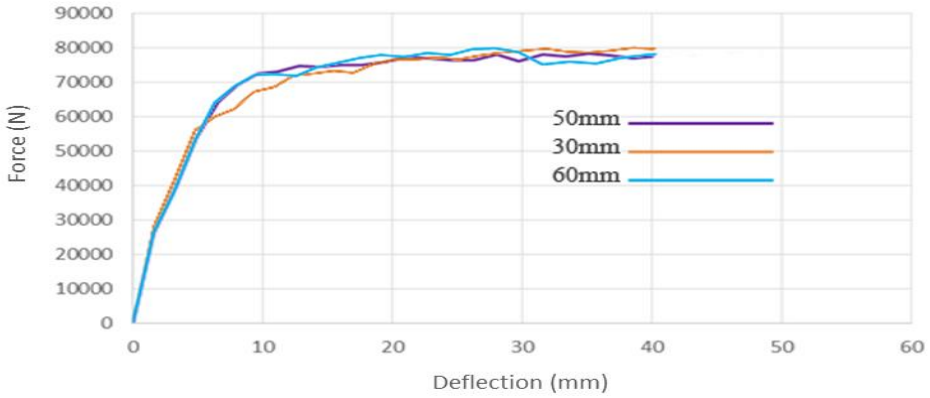

Fig 18. Mesh Sensitivity Analysis

Research findings

The performance of the strengthened models was evaluated based on their yield moment, load-deflection behavior, and energy dissipation capacity.

Flexural Capacity and Yield Moment

The yield moments for all models are summarized in Tables 5, 6 and 7. The Base model had a yield moment of 9.52 kNm. All strengthened models showed a substantial increase in flexural capacity.

The applied prestressing force induces a state of pre-compression in the tension zone of the composite section. This initial compression must be overcome by the applied load before tensile stresses can initiate cracking, thereby significantly increasing the cracking moment of the section. This delay allows for greater utilization of the concrete's compressive strength and postpones the yielding of the main tensile reinforcement, resulting in a substantially higher flexural capacity.

Table 5. 1S Models Yield Moments

Yield Moments (kNm)	Model Name
34.93	1S-300
36.46	1S-600
40.1	1S-900

Table 6. 2S Models Yield Moments

Yield Moments (kNm)	Model Name
36.33	2S-300
42.78	2S-600
48.87	2S-900

Table 7. 3S Models Yield Moments

Yield Moments (kNm)	Model Name
45.04	3S-300
47.65	3S-600
50.33	3S-900

Effect of Prestress Level

For a fixed number of tendons, increasing the prestress level consistently increased the yield moment. For the 1-tendon series (1s), increasing the total prestress from 300 to 900 MPa resulted in a 14.8% increase in yield moment. For the 2-tendon series (2s), the same increase in prestress led to a 34.5% improvement in yield moment. This trend, however, was accompanied by a reduction in ductility, as the load-deflection curves (Figures 19, 20, and 21) show a more brittle response at higher prestress levels.

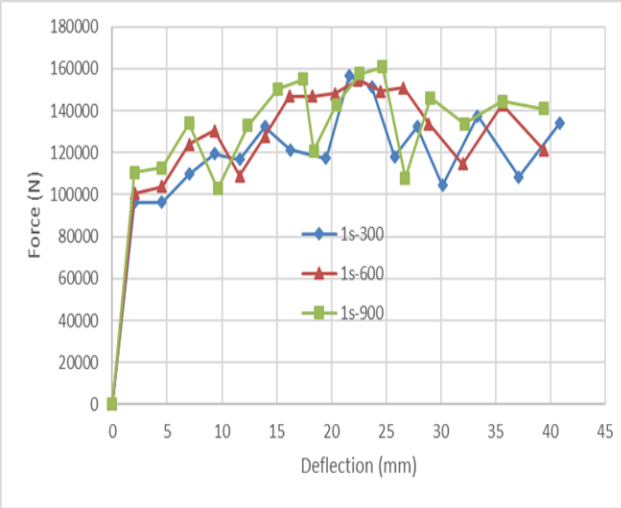

Fig 19. 1S Models Load-Deflection Curves

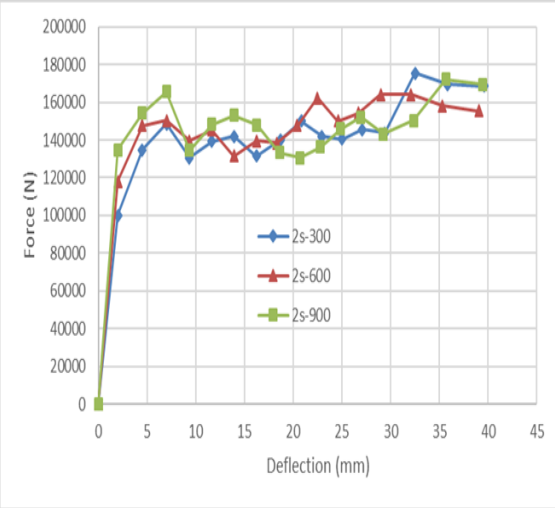

Fig 20. 2S Models Load-Deflection Curves

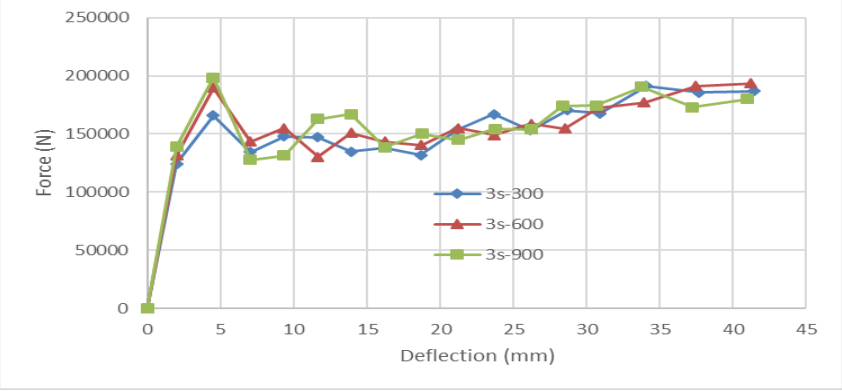

Fig 21. 3S Models Load-Deflection Curves

Effect of Tendon Number

Comparing models with the same total prestress but different numbers of tendons reveals that distributing the force among more tendons improves performance. For a total prestress of 300 MPa, using two tendons (model 2s-300) and three tendons (model 3s-300) increased the yield moment by 4% and 30%, respectively, compared to the single-tendon model (1s-300).

This is likely due to a more uniform distribution of the pre-compressive stress. The highest flexural capacity was achieved by model 3s-900, with a yield moment of 50.33 kNm. This represents a remarkable 428.7% increase compared to the Base model. This result is approximately 2.5 times greater than the enhancement reported for the UHPFRC jacketed beam in the reference study (Lampropoulos et al., 2016), highlighting the significant advantage of incorporating prestressing.

The load-deflection curves for models with the same prestress level but varying tendon numbers are compared in Figures 22, 23, and 24.

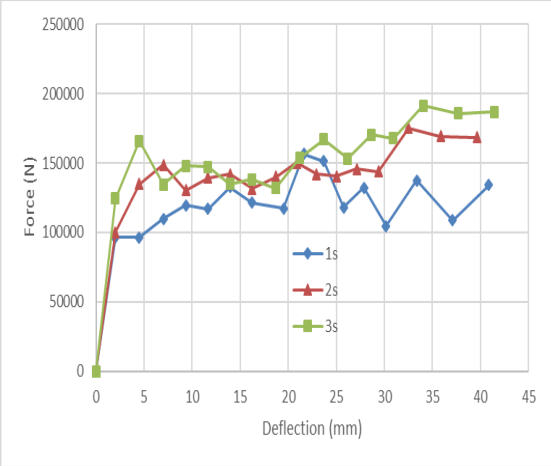

Fig 22. 300 MPa Prestressed Models Load-Deflection Curves

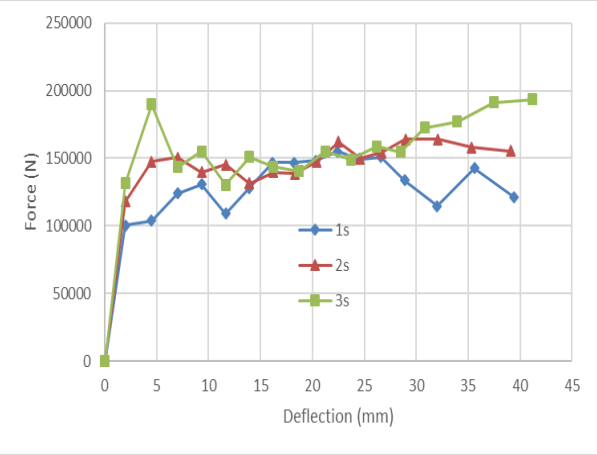

Fig 23. 600 MPa Prestressed Models Load-Deflection Curves

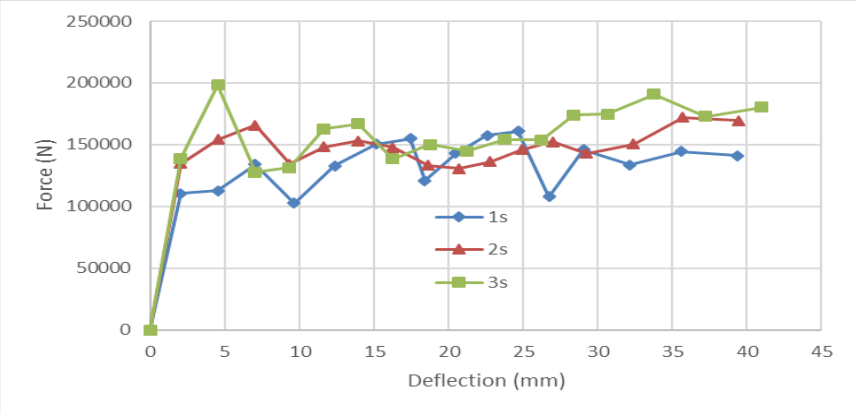

Fig 24. 900 MPa Prestressed Models Load-Deflection Curves

Energy Dissipation

The capacity of a structure to dissipate energy is critical for its performance under seismic loading. Two energy metrics were evaluated: inelastic dissipated energy (ALLPD) and energy dissipated by damage (ALLDMD).

The significant increase in energy dissipation is attributed to the composite action and the controlled, distributed cracking behavior enabled by the prestressed sections. The system is able to undergo larger inelastic deformations before failure, and the damage is spread over a wider area rather than being localized, allowing for greater absorption and dissipation of input energy, which is a critical attribute for seismic resilience.

Inelastic Dissipated Energy

The values are presented in Table 8. The proposed strengthening method increased the inelastic energy dissipation by 15.5% (for model 1s-300) to a maximum of 59.9% (for model 3s-900) compared to the Base model.

Table 8. Inelastic Dissipated Energy

Model Name	Energy (J)	Increase (%)
Base	96587.4	-
1S-300	111606.4	15.5
1S-600	121262.8	25.5
1S-900	133549.5	38.3
2S-300	123851.2	28.2
2S-600	131219.4	35.8
2S-900	142664.8	47.7
3S-300	135104.7	39.9
3S-600	144909.5	50
3S-900	154414.7	59.9

Energy Dissipated by Damage

The values are listed in Table 9. The increase in this metric was even more pronounced, ranging from 49.5% (for model 1s-300) to 191% (for model 3s-900) relative to the Base model.

Table 9. Energy Dissipated by Damage

Model Name	Energy (J)	Increase (%)
Base	6520.9	-
1S-300	8264.7	49.5
1S-600	8436.5	54.4
1S-900	8882.9	67.1
2S-300	11396.9	138.5
2S-600	11626.6	145
2S-900	11656.5	145.9
3S-300	11966.7	154.7
3S-600	12715.9	176
3S-900	13234	191

These results indicate that the proposed method not only strengthens the beam but also substantially improves its ability to dissipate energy, which can help prevent catastrophic failure during severe loading events like earthquakes.

Results

This numerical proof-of-concept study has successfully demonstrated the significant potential of using prefabricated prestressed beams for strengthening RC beams. Based on the Finite Element Analysis (FEA), the following conclusions are drawn:

1. The proposed strengthening method provides a very significant increase in the flexural capacity of RC beams. The maximum observed yield moment increased by 428.7% compared to the unstrengthened base model.
2. Both the level of prestress and the number of tendons are critical parameters. Increasing the prestress level boosts the yield moment but tends to result in more brittle behavior. Distributing the prestressing force among a larger number of tendons leads to a higher cracking moment and better overall performance.
3. The method substantially enhances the energy dissipation capacity of the beams. Inelastic energy dissipation increased by up to 59.9%, and energy dissipated through damage mechanisms increased by up to 191%. This improvement is crucial for seismic resilience.
4. When compared to advanced strengthening techniques like UHPFRC jacketing (Lampropoulos et al., 2016), the proposed method demonstrates superior performance in terms of flexural strength enhancement, largely due to the beneficial effects of prestressing.

Overall, the results confirm that strengthening with prefabricated prestressed concrete sections is a highly effective retrofitting technique. The compelling performance demonstrated in this study strongly justifies experimental research to validate these numerical findings and develop practical guidelines for its implementation.

References

Abbassi, K., Janghorban, M., Javanmardi, F., & Mobasseri, S. (2023). Feasibility study of femur bone with continuum model. *Journal of Medical Engineering & Technology*, *47*(7), 355-366. https://doi.org/https://doi.org/10.1080/03091902.2024.2336512

Abdolpour, H., & Sawicki, B. (2025). Analyzing fracture mechanism of high performance concrete using concrete damage plasticity model. *Archives of Civil and Mechanical Engineering*, *25*(5), 241. https://doi.org/https://doi.org/10.1007/s43452-025-01287-3

Al-Ashmawy, A. M., Shallan, O., Sakr, T. A., & Abd-EL-Mottaleb, H. E. (2023). Numerical investigations of reinforcement concrete beams with different types of FRP bars. *Structural engineering and mechanics: An international journal*, *88*(6), 599-608. https://doi.org/https://doi.org/10.12989/sem.2023.88.6.599

Al Khaffaf, I., Hawileh, R. A., Sahoo, S., Abdalla, J. A., & Kim, J. H. (2025). Toward carbon-neutral construction: A review of zero-carbon concrete. *Journal of Building Engineering*, *99*, 111578. https://doi.org/https://doi.org/10.1016/j.jobe.2024.111578

Althoey, F., Ansari, W. S., Sufian, M., & Deifalla, A. F. (2023). Advancements in low-carbon concrete as a construction material for the sustainable built environment. *Developments in the built environment*, *16*, 100284. https://doi.org/https://doi.org/10.1016/j.dibe.2023.100284

Attari, N., Youcef, Y. S., & Amziane, S. (2019). Seismic performance of reinforced concrete beam–column joint strengthening by frp sheets. *Structures*, *20*, 353-364. https://doi.org/https://doi.org/10.1016/j.istruc.2019.04.007

Bouakaz, K., Daouadji, T. H., Meftah, S., Ameur, M., Tounsi, A., & Bedia, E. A. (2014). A numerical analysis of steel beams strengthened with composite materials. *Mechanics of Composite Materials*, *50*(4), 491-500. https://doi.org/https://doi.org/10.1007/s11029-014-9435-x

Chen, Z., Xu, R., Ling, Z., Liang, Y., Lu, S., & Qin, L. (2023). Experimental and numerical analysis of shear performance of reinforced concrete beams with double openings. *Archives of Civil and Mechanical Engineering*, *23*(3), 195. https://doi.org/https://doi.org/10.1007/s43452-023-00745-0

Elsalakawy, T. S., El-Diasity, M., Mounir Naguib, M., & Hamdy, M. (2025). Effect of vertical irregularity of concrete frame systems on the seismic response modification factor. *Computers and Concrete, An International Journal*, *36*(5), 127-140. https://doi.org/https://doi.org/10.12989/cac.2025.36.2.127

Esmaeeli, E., Barros, J. A., Sena-Cruz, J., Fasan, L., Prizzi, F. R. L., Melo, J., & Varum, H. (2015). Retrofitting of interior RC beam–column joints using CFRP strengthened SHCC: cast-in-place solution. *Composite Structures*, *122*, 456-467. https://doi.org/https://doi.org/10.1016/j.compstruct.2014.12.012

Favier, A., De Wolf, C., Scrivener, K., & Habert, G. (2018). *A sustainable future for the European Cement and Concrete Industry: Technology assessment for full decarbonisation of the industry by 2050*.

Gergely, J., Pantelides, C. P., & Reaveley, L. D. (2000). Shear strengthening of RCT-joints using CFRP composites. *Journal of composites for construction*, *4*(2), 56-64. https://doi.org/https://doi.org/10.1061/(ASCE)1090-0268(2000)4:2(56

Gkournelos, P., Triantafillou, T., & Bournas, D. (2021). Seismic upgrading of existing reinforced concrete buildings: A state-of-the-art review. *Engineering Structures*, *240*, 112273. https://doi.org/https://doi.org/10.1016/j.engstruct.2021.112273

Habibi, M., Mobasseri, S., Zare, A., & Souriaee, V. (2022). Drug delivery with therapeutic lens for the glaucoma treatment in the anterior eye chamber: a numerical simulation. *Biomedical Engineering Advances*, *3*, 100032. https://doi.org/https://doi.org/10.1016/j.bea.2022.100032

Hadi, M. N., & Tran, T. M. (2014). Retrofitting nonseismically detailed exterior beam–column joints using concrete covers together with CFRP jacket. *Construction and Building Materials*, *63*, 161-173. https://doi.org/https://doi.org/10.1016/j.conbuildmat.2014.04.019

Hajihashemi, A. (2008). *Hashemi, A. H. (2008). Strengthening of reinforced concrete beams using prestressed CFRP materials by the near-surface mounted (NSM) method [Master's thesis, Isfahan University of Technology]*. Isfahan University of Technology]. Iran.

Hassani Tabar, H., Salehi YaneSari, M., Hosseinali Beygi, M., & Teymouri Yanehsari, M. (2014). *Experimental investigation of flexural behavior of reinforced concrete beams strengthened with prestressed CFRP plates* 8th National Congress on Civil Engineering, Babol, Iran.

He, C., Yu, Y., Li, G., Zhuge, Y., Zeng, J.-J., & Zhang, M. (2025). Experimental study and finite element simulation of innovative steel buckling restrained braces with three yielding stages. Structures,

International, A. (2018). ASTM A416 / A416M-18, Standard Specification for Steel Strand, Uncoated Seven-Wire for Prestressed Concrete, ASTM International, West Conshohocken, PA,. In. United States.

Islam, A. S. (2020). Computer aided failure prediction of reinforced concrete beam. *Computers and Concrete, An International Journal*, *25*(1), 67-73. https://doi.org/https://doi.org/10.12989/cac.2020.25.1.067

Jankowiak, T., & Lodygowski, T. (2005). Identification of parameters of concrete damage plasticity constitutive model. *Foundations of civil and environmental engineering*, *6*(1), 53-69.

Kabashi, N., Muhaxheri, M., Krasniqi, E., Murati, Y., & Latifi, F. (2025). Advancements in Fiber-Reinforced Polymer (FRP) Retrofitting Techniques for Seismic Resilience of Reinforced Concrete Structures. *Buildings*, *15*(4), 587. https://doi.org/https://doi.org/10.3390/buildings15040587

Karbhari, V. M. (2001). Materials considerations in FRP rehabilitation of concrete structures. *Journal of materials in civil engineering*, *13*(2), 90-97. https://doi.org/https://doi.org/10.1061/(ASCE)0899-1561(2001)13:2(90

Kim, K., Lee, B.-G., Jung, J.-S., & Lee, K.-S. (2025). Seismic performance evaluation of reinforced concrete columns using finite element-based nonlinear dynamic analysis. Structures,

Laib, S., Meftah, S. A., Youzera, H., Ziane, N., & Tounsi, A. (2021). Vibration and damping characteristics of the masonry wall strengthened with bonded fibre composite patch with viscoelastic adhesive layer. *Computers and Concrete*, *27*(3), 253-268. https://doi.org/https://doi.org/10.12989/cac.2021.27.3.253

Lampropoulos, A., Paschalis, S. A., Tsioulou, O., & Dritsos, S. E. (2016). Strengthening of reinforced concrete beams using ultra high performance fibre reinforced concrete (UHPFRC). *Engineering Structures*, *106*, 370-384. https://doi.org/https://doi.org/10.1016/j.engstruct.2015.10.042

Lewiński, P. M., & Więch, P. P. (2020). Finite element model and test results for punching shear failure of RC slabs. *Archives of Civil and Mechanical Engineering*, *20*(2), 36. https://doi.org/https://doi.org/10.1007/s43452-020-00037-x

Ma, C., Wang, D., & Wang, Z. (2017). Seismic retrofitting of full-scale RC interior beam-column-slab subassemblies with CFRP wraps. *Composite Structures*, *159*, 397-409. https://doi.org/https://doi.org/10.1016/j.compstruct.2016.09.094

Mirzaee, A., Torabi, A., & Totonchi, A. (2021). Experimental study on the behavior of reinforced concrete beam boosted by a post-tensioned concrete layer. *Computers and Concrete*, *28*(6), 549-557. https://doi.org/https://doi.org/10.12989/cac.2021.28.6.549

Mobasseri, S., & Janghorban, M. (2024). Non-homogeneous model for studying femur bone implants with considering defects. *International Journal of Modelling and Simulation*, 1-11. https://doi.org/https://doi.org/10.1080/02286203.2024.2392217

Mobasseri, S., Karami, B., Sadeghi, M., & Tounsi, A. (2022). Bending and torsional rigidities of defected femur bone using finite element method. *Biomedical Engineering Advances*, *3*, 100028. https://doi.org/https://doi.org/10.1016/j.bea.2022.100028

Mobasseri, S., & Mobasseri, M. (2016, 2016/7/28). *A Comparative Study Between ABS and Disc Brake System Using Finite Element Method* International Conference on researches in Science and Engineering, Turkey.

Mobasseri, S., Sadeghi, M., Janghorban, M., & Tounsi, A. (2020). Approximated 3D non-homogeneous model for the buckling and vibration analysis of femur bone with femoral defects. *Biomaterials and Biomechanics in Bioengineering*, *5*(1), 25-35. https://doi.org/https://doi.org/10.12989/bme.2020.5.1.025

Mobasseri, S., & Soltani, H. (2013). Impact of driving style on fuel consumption. *Nature and Science*, *11*, 87-89.

Mobasseri, S., Zare, A., & Janghorban, M. (2024). Dynamic behavior of dragonfly wing veins including the role of hemolymph. *Journal of Mechanics in Medicine and Biology*, *24*(04), 2350093. https://doi.org/https://doi.org/10.1142/S0219519423500938

Nawy, E. G. (1988). *Prestressed concrete. A fundamental approach*. Prentice Hall.

Ni, Y., Ma, Y., Lin, H., Zhang, H., & Zhuo, Y. (2025). Finite element model updating of existing bridge structures based on measured data and deep learning method. Structures,

Raza, S., Khan, M. K., Menegon, S. J., Tsang, H.-H., & Wilson, J. L. (2019). Strengthening and repair of reinforced concrete columns by jacketing: State-of-the-art review. *Sustainability*, *11*(11), 3208. https://doi.org/https://doi.org/10.3390/su11113208

Sadeghi, V., & Hesami, S. (2018). Finite element investigation of the joints in precast concrete

pavement. *Computers and Concrete, An International Journal*, *21*(5), 547-557. https://doi.org/https://doi.org/10.12989/cac.2018.21.5.547

Shahbazpanahi, S., & Manie, S. (2006). *A review of strengthening methods for reinforced concrete beams* 1st National Conference on Urban Civil Engineering, Sanandaj, Iran.

Shakor, P., Gowripalan, N., & Rasouli, H. (2021). Experimental and numerical analysis of 3D printed cement mortar specimens using inkjet 3DP. *Archives of Civil and Mechanical Engineering*, *21*(2), 58. https://doi.org/https://doi.org/10.1007/s43452-021-00209-3

Sharif, A., Al-Sulaimani, G., Basunbul, I., Baluch, M., & Ghaleb, B. (1994). Strengthening of initially loaded reinforced concrete beams using FRP plates. *Structural Journal*, *91*(2), 160-168.

Singh, S. B., & Murty, C. (2024). *RC Structures Strengthened with FRP for Earthquake Resistance*. Springer. https://doi.org/https://doi.org/10.1007/978-981-97-0102-5

Sümer, Y., & Aktaş, M. (2015). Defining parameters for concrete damage plasticity model. *Challenge Journal of Structural Mechanics*, *1*(3), 149-155. https://doi.org/https://doi.org/10.20528/cjsmec.2015.07.023

Systèmes, D. (2016). Abaqus 2016 Documentation.© Dassault Systemes. In.

Tan, J.-K., Zheng, W.-L., Wang, Y.-H., Su, M.-N., Zhao, L., Zhang, Y.-H., Feng, Y., & Chen, D.-X. (2025). Finite element modelling and design of concrete wind turbine towers subjected to combined compression and bending. Structures,

Wang, B., Chen, P., Jiang, H., & Wang, J. (2024). Performance of steel-plate-reinforced concrete composite walls in tall structures. *Proceedings of the Institution of Civil Engineers-Civil Engineering*, *177*(3), 118-125. https://doi.org/https://doi.org/10.1680/jcien.23.00167

.